https://doi.org/10.26565/2220-637X-2025-44-06 ISSN 2220-637X
УДК: 577.332

STUDYING LIGAND-PROTEIN INTERACTIONS IN THE ERA OF ARTIFICIAL INTELLIGENCE: BENCHMARKING BOLTZ-1 FOR 3D-STRUCTURE PREDICTION OF BIOMOLECULAR COMPLEXES

M. V. Prud[*†,a], A. Kyrychenko[*b]

[*]*V. N. Karazin Kharkiv National University, School of Chemistry, 4 Svobody sqr., Kharkiv, 61022 Ukraine*
[†]*Enamine Ltd., Winston Churchill Street 78, Kyiv 02094, Ukraine*

a) mykyta.prud@gmail.com https://orcid.org/0000-0002-0051-8104
b) a.v.kyrychenko@karazin.ua https://orcid.org/0000-0002-6223-0990

Modeling ligand-protein interactions is essential in various scientific and industrial applications, especially in drug discovery and structural biology. In the past year, several AI-driven computational tools, such as AlphaFold 3 and Chai-1r, have revolutionized the field of biomolecular structure prediction. Most recently, an open-source deep learning model called Boltz-1 has also been introduced, marking a significant advancement in biomolecular interaction modeling. To assess the performance of Boltz-1 in comparison to other computational tools, we benchmarked its capability to accurately reproduce the 3D structures of various biomolecular complexes. These complexes included essential enzymes and ligands of varying complexities, such as low-molecular organic ligands, sterols, and peptidomimetics. We found that Boltz-1 demonstrated strong performance in reproducing protein folding, achieving a root mean square deviation (RMSD) of less than 1 Å. When compared to other computational tools, such as Glide by Schrödinger and AutoDock Vina, Boltz-1's ability to predict the 3D structures of biomolecular complexes was well balanced. It successfully re-docked a diverse set of ligands with varying complexities, achieving binding poses that were comparable to those of the commercial software Glide. In terms of a RMSD and ligand-binding ranking, Boltz-1 outperformed the widely used docking tool AutoDock Vina for all evaluated ligands, creating opportunities to enhance computational screening of ligand-protein interactions.

Keywords: protein folding, ligand-protein interaction, drug design, artificial intelligence, Boltz-1.

Introduction

Understanding how small molecules (ligands) interact with proteins is fundamental to designing effective drugs. Modeling these interactions helps identify potential drug candidates that can bind to specific protein targets, inhibiting or activating their functions to treat diseases [1-3]. By predicting the 3D structure of ligand-protein complexes, researchers can optimize the design of compounds to improve binding affinity, selectivity, and other pharmacological properties [4-6]. This approach accelerates the drug development process and reduces costs.

Boltz-1 is an open-source deep learning model designed to predict the 3D structures of biomolecular complexes, including interactions between proteins and ligands [7]. Boltz-1 achieves AlphaFold3-level accuracy in predicting biomolecular structures, making it a powerful tool for modeling complex interactions involving proteins, RNA, DNA, and other molecules. It demonstrates strong performance in predicting protein-ligand interactions, with a notable LDDT-PLI score of 65%, outperforming Chai-1, which is another open-source AI model developed for predicting molecular structures and interactions.

The Boltz-1 model supports a wide range of molecular interactions, including modified residues, covalent ligands, and glycans. It can also condition predictions on specified interaction pockets or contacts, enhancing its flexibility in modeling diverse biomolecular complexes. It demonstrates particularly strong protein-ligand and protein-protein performance. The model's ability to accurately predict ligand-protein binding interactions is crucial for drug discovery and therapeutic design, as it helps in understanding and designing molecular interactions at a detailed level.

Boltz-1 combines open-source accessibility with performance comparable to proprietary tools, making it a groundbreaking resource in structural biology. Fig. 1 illustrate a typical pipeline of Botlz-1 processing. It accepts FASTA files, YAML schemas, or directories for batch processing, simplifying integration into diverse workflows. It outputs five predicted 3D structures of the ligand-protein complex in CIF format.

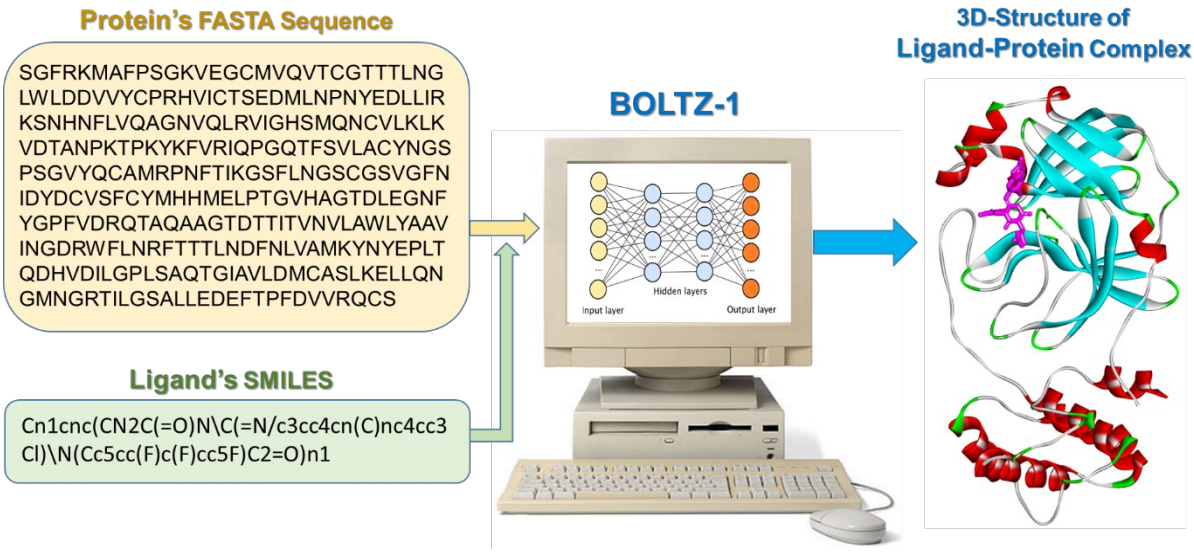

Figure 1. The typical Boltz-1 pipeline scheme illustrates how Boltz-1 processes input data. It accepts a primary protein structure in FASTA sequence format along with a ligand's 2D structure provided in SMILES notation. The output files include up to five predicted 3D structures of the ligand-protein complex in CIF format, accompanied by corresponding confidence metrics.

By democratizing high-precision biomolecular modeling, Boltz-1 promises to accelerate drug discovery, enzyme engineering, and systems biology research. However, Boltz-1's performance in predicting the correct ligand-protein binding mode has not been well demonstrated yet, which limits its broad use among the biomolecular computational community. To address this gap, we assessed Boltz-1's ability to predict the 3D structure of various ligand-protein complexes. Our primary focus was to select a series of structurally diverse ligands, spanning range from drug-like heterocyclic molecules, containing multiple branches and macrocyclic moieties, up to sterols and peptidomimetics

Computational Methods

To reproduce the ligand positions from X-ray structures using orthodox methods, we applied two approaches: redocking with the publicly available free AutoDock Vina software and redocking in the Schrödinger Maestro software package using the Glide module.

For the first approach, the molecular docking setup was carried out with the AutoDock Tools (ADT) software, version 1.5.7 [8]. The geometry of the ligands was prepared from its co-crystallized structure with the protein. The ligand structure was conformationally flexible, so that all possible rotations around torsional angles were allowed. The addition of hydrogen, the calculation of the Gasteiger charges of the receptor, and ligands were also performed using the ADT software. Molecular docking calculations were performed with the AutoDock Vina 1.1.2 software [9]. For each complex, one docking calculation was performed with exhaustiveness of 8, which generated 9 docking poses.

In the second case, the Schrödinger Maestro software package version 2024-1 was employed. The targets were prepared using the Protein Preparation Wizard [10], which involved removing solvent molecules and adding missing hydrogen atoms. Protein structure optimization was carried out in "Simplified Rules" mode at neutral pH. The energy of the protein structure was minimized using the OPLS4 force field [11]. Ligand preparation was conducted using the LigPrep module, followed by minimization with the OPLS4 force field. The Epik Classic submodule was utilized to reproduce the correct protonation state under biological conditions. The Receptor Grid Generation module was then used to create the binding site, and redocking was performed using Glide SP [12-15].

Boltz-1 was accessed via the web version available on the TamarindBio website (https://app.tamarind.bio/boltz, Version 0.4.0). The number of predicted samples was set to 5, while all other settings remained at their default values.

The PyMOL Molecular Graphics System, Version 3.0 Schrödinger, LLC was used for visualization and RMSD analysis.

Results and Discusion

To evaluate the performance of Boltz-1, we selected a series of ligand-protein complexes with known X-ray structures available in the Protein Data Bank (PDB) that involve essential enzymes and small ligands. Considering that the studied Boltz model was trained on public PDB data available until November 2024, our benchmarking set also included some structures published after that. The main metrics used for assessment include the root mean square deviation (RMSD), which quantifies the difference between predicted and experimental structures of the protein and its bound ligand. Additionally, we assessed the accuracy and reliability of binding affinity predictions by evaluating two popular molecular docking scoring functions: Schrödinger Glide and AutoDock Vina.

Main protease M^{pro} of SARS-CoV-2 virus in complex with Ensitrelvir. The main protease, known as M^{pro} (a 3C-like protease), is responsible for cleaving eleven specific sites on the two SARS-CoV-2 polyproteins. M^{pro} is comprised of three domains: a chymotrypsin-like domain (Domain I), a 3C-protease-like domain (Domain II), and a third domain (Domain III) that contains five α-helices [16]. The binding pocket of M^{pro} is situated between Domains I and II and features a catalytic Cys-His dyad, consisting of Cys145 and His41 [17-18]. Therefore, M^{pro} has attracted essential attention and is considered an ideal target for developing antiviral agents [19-23].

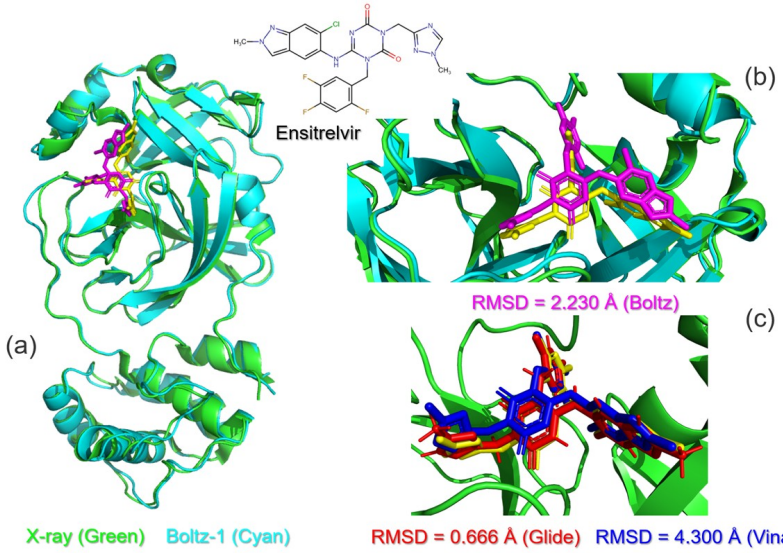

Figure 2. (a) Boltz-1`s prediction of the 3D-structure of the ligand-protein complex between the main protease M^{pro} of the SARS-CoV-2 virus and co-crystalized non-covalent inhibitor S-217622 (Ensitrelvir). The X-ray structures of M^{pro} was obtained from PDB ID: 8HEF [24]. (b) The detailed overlap of the X-ray and Boltz-1 estimated binding modes of Ensitrelvir at M^{pro} pocket. (c) Comparison of the X-ray binding mode of Ensitrelvir at M^{pro} pocket (yellow) with molecular docking calculations using Glide (*red*) and AutoDock Vina (*blue*).

Non-peptide oral drug called ensitrelvir has received approval for sale in Japan on November 22, 2022. Ensitrelvir showed significant inhibitory activity against SARS-CoV-2 M^{pro} as a non-covalent non-peptide inhibitor [24-25]. Figure 2 illustrates the performance of Botlz-1 in predicting the fold of the M^{pro} protease and the binding mode of Ensitrelvir. The predicted M^{pro} fold matches the known X-ray structure remarkably well, with RMSD value as low as 0.806 Å (see Fig. 2a and Table 1). Additionally, the binding conformation of Ensitrelvir was accurately captured, yielding a RMSD of 2.230 Å (Fig. 2b), which is close to the best-predicted pose determined by Glide, with a RMSD of 0.666 Å (Fig. 2c).

Peroxisome Proliferator-Activated Receptor Delta (PPARδ). Peroxisome Proliferator-Activated Receptors (PPARs) are a class of nuclear receptor proteins that act as transcription factors to regulate the expression of genes associated with various cellular processes [26].

Recently, high-throughput screening combined with X-ray analysis has revealed that some sulfonylthiadiazole derivatives exhibit an unusual binding mode at both PPARγ and PPARδ receptors. The ligand WLM has demonstrated partial dual action as an agonist, showing high potency and *in vivo* efficacy (Fig. 3a). It selectively binds to PPARδ, characterized by an EC_{50} of 738 nM [27]. Therefore, the PPARδ-WLM complex presents a challenging system for the Boltz-1 benchmark.

Figure 3 illustrates the benchmarking of the Boltz-1 method for the PPARδ-WLM complex. The 3D structure of the ligand-binding domain (LBD) of PPARδ was accurately reconstructed by Boltz-1, achieving a protein RMSD of 0.853 Å (see Fig. 3a and Table 1). Additionally, the binding conformation of the conformationally flexible ligand WLM was perfectly reproduced, with a RMSD of 0.688 Å (Fig. 3b), which is the best result currently in the field (Fig. 3c). In contrast, docking with Autodock Vina failed to replicate the correct binding mode for WLM (Fig. 3c).

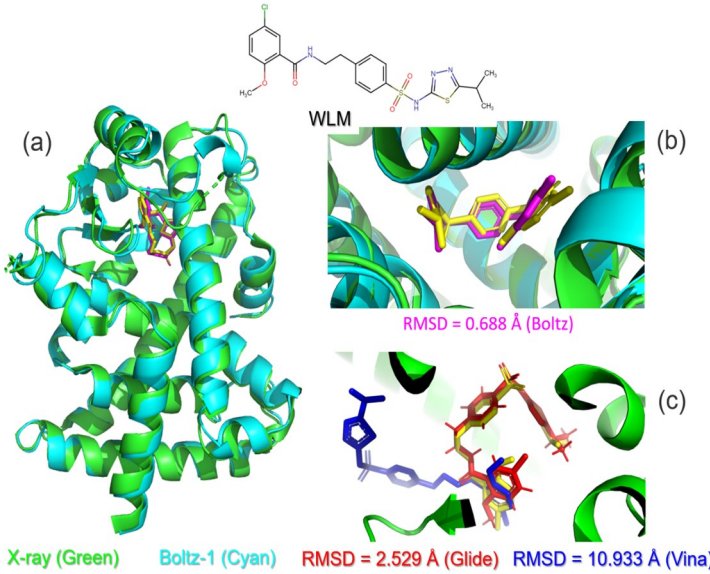

Figure 3. (a) Boltz-1`s prediction of the 3D-structure of the ligand-protein complex between the PPARδ LBD and the ligand WLM. The X-ray structures of PPARδ estimated at a resolution of 2.3 Å was obtained from PDB ID: 2XYJ [27]."(b) The detailed overlap of the X-ray and Boltz-1 estimated binding modes of WLM at PPARδ. (c) Comparison of the X-ray binding mode of WLM at PPARδ (*yellow*) with molecular docking calculations using Glide (*red*) and AutoDock Vina (*blue*).

Table 1. Summary of Boltz-1 predictions for the 3D structure of ligand-protein complexes in relation to their X-ray structures (PDB ID). The binding mode of the ligand was also compared with molecular docking calculations performed using Schrödinger Glide and AutoDock Vina.[a, b]

PDB ID	Boltz-1			Glide		AutoDock Vina	
	Score	Protein RMSD, Å	Ligand RMSD, Å	docking score	Ligand RMSD, Å	Binding affinity, kcal/mol	Ligand RMSD, Å
8HEF	0.939	0.806	2.230	-9.6	0.666	-9.1	4.300
2XYJ	0.934	0.853	0.688	-9.0	2.529	-9.7	10.933
2YXJ	0.867	1.188	1.410	-12.1	1.340	-10.2	12.370
1HPV	0.975	0.483	6.080	-8.1	0.953	-6.1	20.970
8P81	0.909	1.683	2.096	-11.2	1.427	-6.8	8.461
3UUD	0.963	0.724	0.472	-10.9	0.621	-11.2	0.540
6OQB	0.963	0.505	0.528	-9.6	2.672	-8.5	5.985
6Z54	0.951	0.557	1.108	-5.0	9.680	-8.7	6.730
8VVE	0.779	2.216	7.356	-7.3	1.409	-10.9	6.694
5JM4	0.731	0.901	5.607	-7.7	10.653	-6.6	10.466

a – the smallest RMSD corresponding to the best-predicted mode is highlighted in yellow.
b – note, the Boltz score does not in any way describe the pose of the ligand, but only reflects the model's confidence in reproducing the protein structure.

Bcl-xL in complex with ABT-737. B-cell lymphoma-extra large (Bcl-xL) is a protein encoded by the BCL2L1 gene and belongs to the Bcl-2 family of proteins. Bcl-xL is primarily recognized for its anti-apoptotic properties, which means it prevents programmed cell death [28-29]. Specifically, it inhibits the release of mitochondrial contents such as cytochrome C, a crucial step in the apoptosis pathway [30-31]. By doing so, Bcl-xL helps maintain the integrity of the mitochondrial membrane, thereby preventing cell death [32-33]. Ligand ABT-737 mimics the BH3 domains of BH3-only proteins and

has potential as anti-cancer therapeutics (Fig. 4a) [34]. Therefore, understanding the precise molecular structure of ABT-737 in Bcl-xL may clarify why it binds strongly to the Bcl-2 pro-survival proteins but fails to interact with the related target Mcl-1.

Figure 4 and Table 1 summarize the benchmarking results of the Boltz-1 method applied to the Bcl-xL:ABT-737 complex. The three-dimensional structure of Bcl-xL was accurately reconstructed by Boltz-1, achieving a RMSD of 1.188 Å. However, the prediction score was relatively low at 0.867, which indicates challenges in accurately modeling the flexible loops (see Fig. 4a).

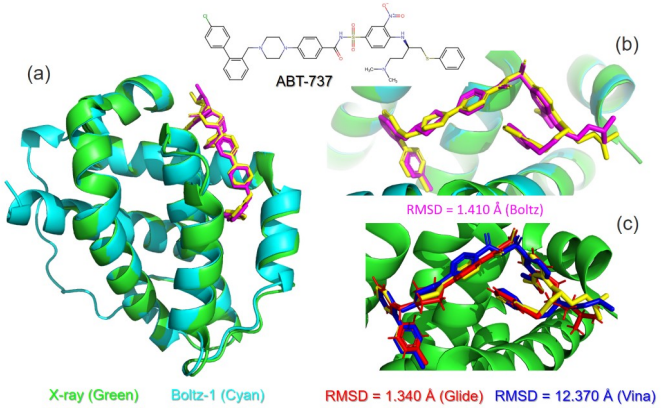

Figure 4. (a) Boltz-1`s prediction of the 3D-structure of the ligand-protein complex between the Bcl-xL and the ligand ABT-737. The X-ray structures of Bcl-xL, acquired a resolution of 2.2 Å, was obtained from PDB ID: 2YXJ [34]. (b) The detailed overlap of the X-ray and Boltz-1 estimated binding modes of ligand ABT-737 at Bcl-xL pocket. (c) Comparison of the X-ray binding mode of ABT-737 at Bcl-xL pocket (*yellow*) with molecular docking calculations using Glide (*red*) and AutoDock Vina (*blue*).

The binding conformation of the conformationally flexible ligand ABT-737 was also well reproduced, resulting in a RMSD of 1.410 Å (Fig. 4b). This result is quite similar to the 1.340 Å RMSD predicted by Glide (Fig. 4c). Autodock Vina, on the other hand, was able to capture the crystal pose of ligand ABT-737 but placed the ligand in the reverse orientation, leading to a significantly higher RMSD of 12.370 Å (Fig. 4c).

Hiv-1 protease in complex with ligand VX-478. The HIV-1 protease is an enzyme crucial for the life cycle of the human immunodeficiency virus type 1 (HIV-1) (Fig. 5a), which causes AIDS [35].

Boltz-1 performed well in reproducing the native fold of the HIV-1 protease, achieving a RMSD of 0.483 Å and the best prediction score of 0.975 (see Fig. 5a and Table 1). However, it faced significant challenges in accurately recovering the binding pose of the ligand VX-478, as shown by a large RMSD of 6.080 Å (Fig. 5b). In contrast, the ligand binding test was successfully passed by Glide, which recorded an impressive RMSD of 0.953 Å (Fig. 5c), while AutoDock Vina completely failed in this aspect.

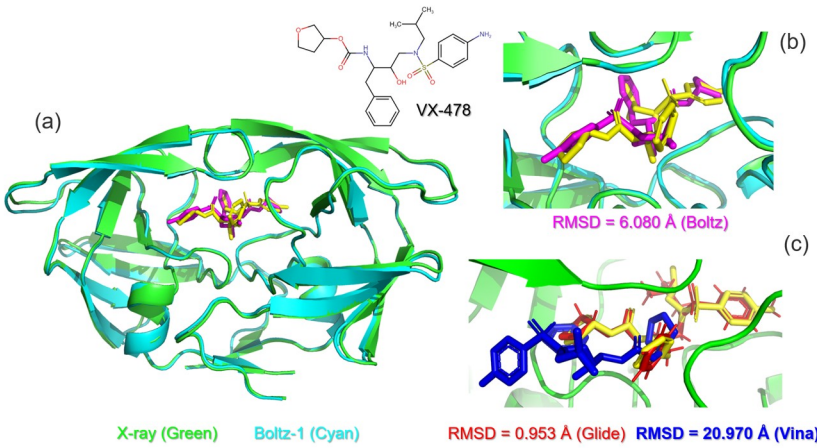

Figure 5. (a) Boltz-1`s prediction of the 3D-structure of the ligand-protein complex between the Hiv-1 protease and the ligand VX-478. The X-ray structure of Hiv-1 protease, measured at resolution of 2.2 Å, was obtained from PDB ID: 1HPV [36]. (b) The Panel illustrates the detailed overlap between the X-ray binding mode and the binding mode estimated by Boltz-1 for VX-478 at the HIV-1 pocket. (c) Comparison of the X-ray binding mode

of VX-478 at the HIV-1 pocket (*yellow*) with molecular docking calculations using Glide (*red*) and AutoDock Vina (*blue*).

Human cyclin-dependent kinase 12 in complex with inhibitor SR-4835. Human Cyclin-Dependent Kinase 12 (CDK12) is a serine/threonine kinase that forms an active complex with Cyclin K (CycK). This complex is essential for transcriptional regulation, maintaining genome stability, and has a significant role in cancer biology. CDK12 consists of a central kinase domain and a unique C-terminal extension, both of which are crucial for ATP binding and its catalytic activity [37].

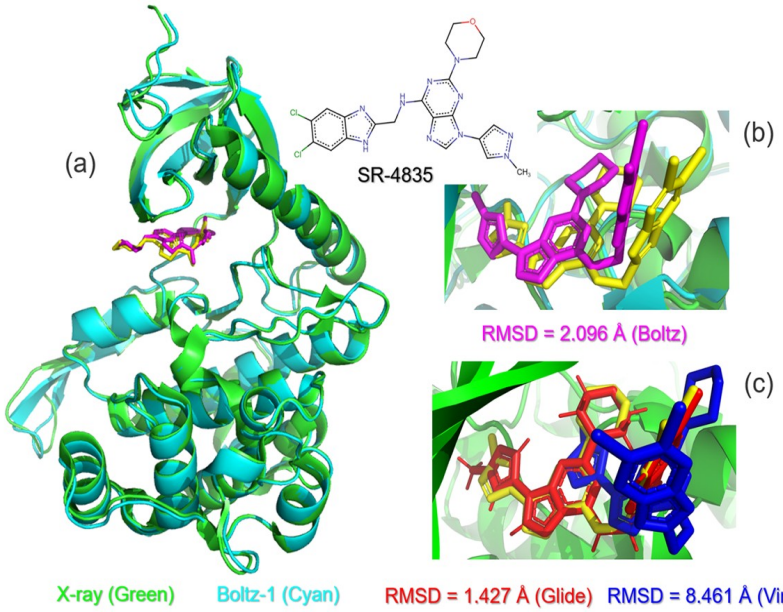

Figure 6. (a) Boltz-1`s prediction of the 3D-structure of the ligand-protein complex between human CDK12 and the inhibitor SR-4835. The X-ray structures of human CDK12, measured at a resolution of 2.68 Å, was obtained from PDB ID: 8P81 [37]. (b) The detailed overlap of the X-ray and Boltz-1 estimated binding modes of ligand SR-4835 at CDK12 pocket. (c) Comparison of the X-ray binding mode of SR-4835 at CDK12 pocket (*yellow*) with molecular docking calculations using Glide (*red*) and AutoDock Vina (*blue*).

Understanding the binding interactions between CDK12 and small-molecule inhibitors is crucial for elucidating its structure-function relationships. As a result, CDK12 has emerged as a promising target for various computational chemistry tools, including docking, *in silico* screening, and deep learning-based design of novel therapeutic agents [38-39].

SR-4835 is a reversible ATP-competitive inhibitor of CDK12 and CDK13. It reduces phosphorylation of RNA Polymerase II (specifically at Ser2 in RPB1) and inhibits transcription elongation [37, 40-41]. Unlike other inhibitors, SR-4835 functions as a molecular glue [42]. Recent crystallographic studies have shown that SR-4835 binds to CDK12/cyclin K in a noncanonical conformation (Fig. 6a-b) [37]. Its benzimidazole component forms hydrogen bonds with the kinase hinge region, while the altered glycine-rich loop and inward αC-helix help stabilize the binding interaction.

Despite the complex 3D structure of CDK12, Botlz-1 successfully recovered its native fold with a RMSD of 1.683 Å (see Fig. 6a). In contrast, the relatively rigid conformation of the inhibitor SR-4835 posed challenges for accurately recovering the X-ray data across all considered scoring methods, with Glide demonstrating slightly better performance (refer to Table 1 and Figs. 6b-c).

Human estrogen receptors (ER) alpha in complex with estradiol. Estrogen receptor alpha (hERα) is a nuclear receptor protein that is activated by the sex hormone estrogen. ERα functions as a ligand-activated transcription factor and is made up of several important domains responsible for hormone binding, DNA binding, and transcription activation. It primarily acts as a chromatin-binding protein and is encoded by the ESR1 gene in humans [43].

Figure 7 presents a summary of the benchmarking results for the complex formed between hERα and estradiol. Notably, Boltz-1 successfully reproduced both the protein folding and ligand binding poses, achieving a RMSD of 0.724 Å for the protein and 0.472 Å for the ligand (see Fig. 7a-b and Table 1). In terms of docking score ranking, Boltz-1 outperformed both Glide and Autodock Vina, which

also produced commendable results, with corresponding RMSD values of 0.621 Å and 0.540 Å (Fig. 7c), respectively.

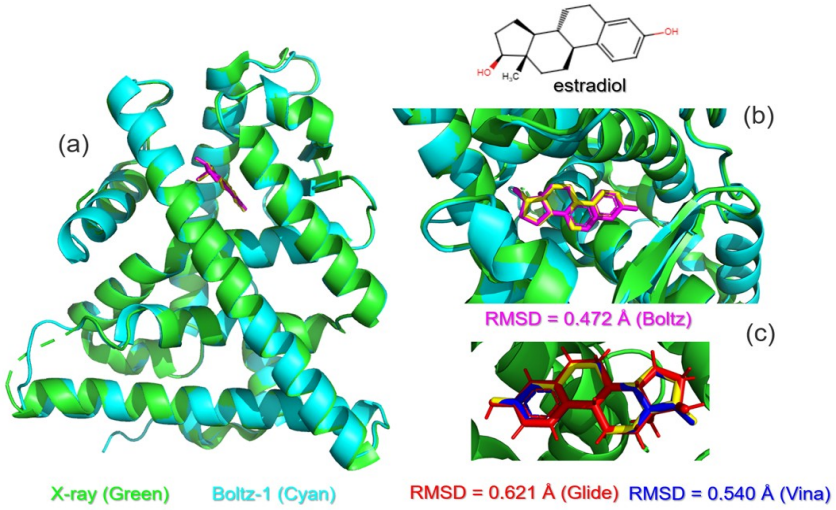

Figure 7. (a) Boltz-1`s prediction of the 3D-structure of the ligand-protein complex between the hERα-LBD and estradiol. The X-ray structures of hERα-LBD (1.6 Å resolution) was obtained from PDB ID: 3UUD [44]. (b) The detailed overlap of the X-ray and Boltz-1 estimated binding modes of ligand estradiol within the hERα-LBD pocket. (c) Comparison of the X-ray binding mode of estradiol within the hERα-LBD pocket (*yellow*) with molecular docking calculations using Glide (*red*) and AutoDock Vina (*blue*).

Myeloid Cell Leukemia-1 in complex with AMG 176. MCL1 is a protein encoded by the MCL1 gene in humans. It belongs to the pro-survival BCL2 family and is often dysregulated in cancer. To address the significant challenges associated with inhibiting MCL1 protein-protein interactions, small-molecule conformational restriction methods, such as those involving ligand AMG 176, are rigorously applied [45].

The biomolecular complex between MCL1 and the ligand AMG 176 was chosen for benchmarking due to the flexible macrocyclic structure and spiro-carbon atom of the ligand, which often present challenges for many scoring algorithms. Surprisingly, Boltz-1 performed exceptionally well, reproducing the ligand binding conformation with a RMSD as small as 0.528 Å (Fig. 8a-b). The protein's 3D structure was also accurately recovered, with a RMSD of 0.505 Å. In comparison, Glide and AutoDock Vina exhibited a decline in binding prediction performance, as indicated by larger RMSD values of 2.672 Å and 5.985 Å, respectively (Fig. 8c). It suggests that Boltz-1 performs better for docking ligands with flexible macrocycles.

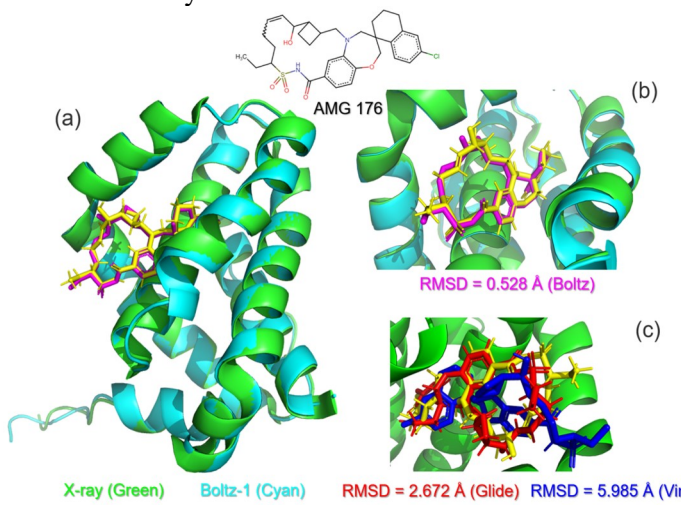

Figure 8. (a) Boltz-1`s prediction of the 3D-structure of the ligand-protein complex between MCL1 and the ligand AMG 176. The X-ray structures of MCL1 (1.6 Å resolution) was obtained from PDB ID: 6OQB [45]. (b) The overlap of the X-ray and Boltz-1 estimated binding modes of the ligand AMG 176 within the MCL1 pocket. (c) Comparison of the X-ray binding mode of the ligand AMG 176 (*yellow*) with molecular docking calculations by Glide (*red*) and AutoDock Vina (*blue*).

CDC-Like Kinase 3 in complex with ligand ODS2003178. CLK3 is a dual-specificity protein kinase that plays a vital role in regulating RNA splicing. It phosphorylates serine/arginine-rich (SR) proteins, which are essential components of the spliceosomal complex. This phosphorylation regulates the activity of SR proteins, influencing the splicing of pre-mRNA and ultimately affecting gene expression [46].

The crystal structure of the dual-specificity protein kinase CLK3 in complex with the macrocyclic ligand ODS2003178 has been determined and is available in the Protein Data Bank under the accession code 6Z54 (Fig. 9a). The structure was solved using X-ray diffraction, providing valuable insights into the binding interactions between CLK3 and ODS2003178. This structure may be valuable for drug design aimed at targeting this kinase [47]. Many inhibitors target multiple kinases, including CLK1, CLK2, and PI3K [48], making it challenging to find selective inhibitors for CLK3. In this context, the ligand identified as ODS2003178 is a macrocyclic compound that serves as a promising candidate for benchmarking (Fig. 9a). This type of scaffold poses a well-known challenge for many online predictors of ligand-protein interactions, as well as for popular molecular docking software like AutoDock Vina.

The biomolecular complex formed between CLK3 and a macrocyclic ligand ODS2003178 presents another challenging example of cyclic ligands. In this case, Boltz-1 performed also very well, achieving a RMSD as low as 1.108 Å for the bound ligand conformation (Fig. 9a-b). Similarly to the above described cyclic AMG 176, Glide and Autodock Vina systematically declined in their performance, as seen by unusually more significant RMSD values of 9.680 Å and 6.730 Å, respectively (Fig. 9c).

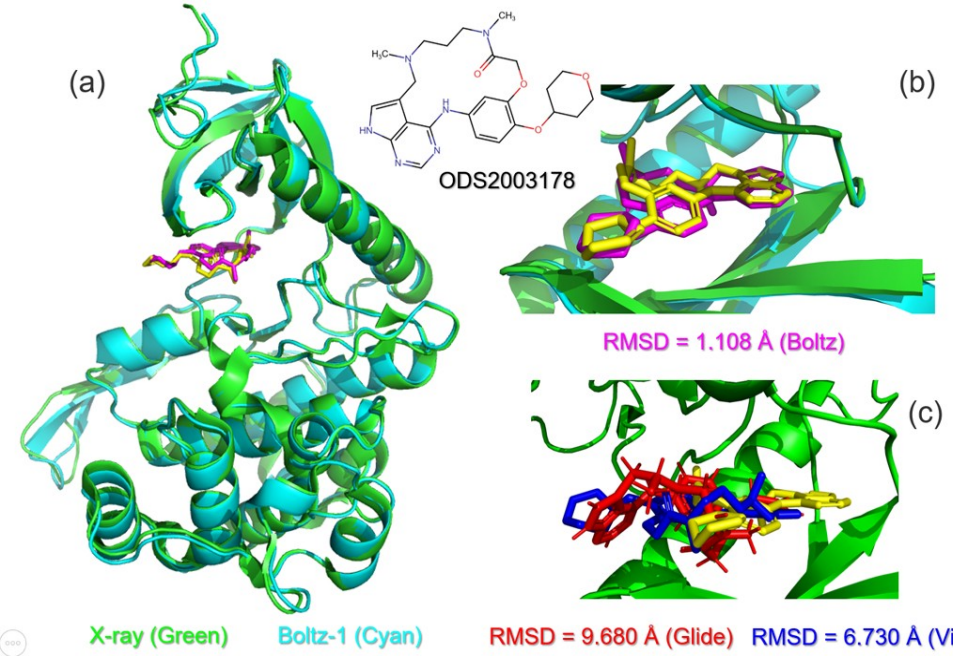

Figure 9. (a) Boltz-1`s prediction of the 3D-structure of the ligand-protein complex between CLK3 and the macrocyclic ligand ODS2003178. The X-ray structures of the enzyme CLK3, measured at a resolution of 1.73 Å, was obtained from PDB ID: 6Z54. (b) The overlap of the X-ray and Boltz-1 estimated binding modes of the ligand ODS2003178 within the CLK3 pocket. (c) Comparison of the X-ray binding mode of the ligand ODS2003178 (*yellow*) with molecular docking calculations by Glide (*red*) and AutoDock Vina (*blue*).

Kappa-opioid receptor-G protein in complex with inverse agonist norBNI. κ-Opioid receptors (KOR), a subfamily of G protein-coupled receptors (GPCRs), are crucial therapeutic targets. In the standard GPCR activation model, the binding of an agonist is necessary for the formation of the receptor–G protein complex, while antagonists inhibit G protein coupling. Therefore, KOR is an important target for *in silico* screening, molecular docking and drug discovery for pain and depression therapeutics [49-50].

Very few potent selective KOR antagonists are known to date, making the discovery of novel, promising candidates for the treatment of opioid addiction of tremendous importance [51-52]. NorBNI (norbinaltorphimine) is a synthetic organic compound composed of two naltrexone moieties with in-

version symmetry, which is classified as a highly selective KOR inverse agonist and antagonist (Fig. 10). NorBNI is a key ligand in opioid research, providing valuable insights into the role of KOR in neuropsychiatric disorders [53]. It is primarily used in scientific studies to investigate KOR's involvement in pain, addiction, mood disorders, and stress responses [54]. Although NorBNI was one of the first identified KOR-selective antagonists, the X-ray structure of its complex with KOR was only released last year (PDB ID: 8VVE) (Fig. 10a) [55]. This makes it an ideal model for our benchmarking, as it falls outside the PDB training dataset of Boltz-1.

The structure prediction of the complex between KOR and the inverse agonist norBNI presents challenges for many computational algorithms due to the unique characteristics of both components: the protein structure is dominated by long α-helices, while the ligand norBNI is a rigid polycyclic compound. In this context, Botlz-1 successfully predicts KOR folding with an acceptable accuracy level, achieving a RMSD of 2.216 Å, although it has one of the lowest prediction scores among the proteins studied, with a score of 0.779 (see Table 1 and Fig. 10a). On the other hand, the prediction of ligand binding accuracy was also low, with an RMSD of 7.356 Å (see Fig. 10b). Despite the complex 3D structure of norBNI, the Glide module effectively predicted its binding mode, resulting in a much lower RMSD of 1.409 Å (see Fig. 10c).

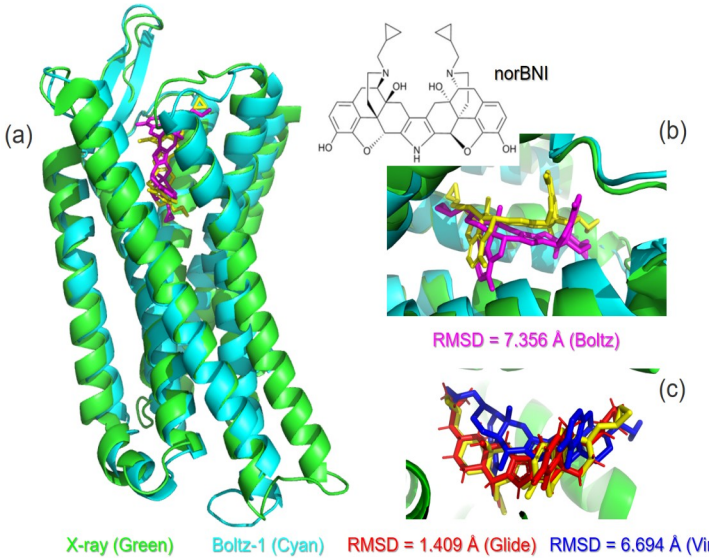

Figure 10. (a) Boltz-1`s prediction of the 3D-structure of the ligand-protein complex between KOR and an inverse agonist norBNI. The Cryo-EM structures of KOR, measured at a resolution of 3.3 Å, was obtained from PDB ID: 8VVE [55]. (b) The overlap of the Cryo-EM and Boltz-1 estimated binding modes of the ligand norBNI within the KOR pocket. (c) Comparison of the Cryo-EM binding mode of the ligand norBNI (*yellow*) with molecular docking calculations by Glide (*red*) and AutoDock Vina (*blue*).

Protein 14-3-3ξ in a complex a peptide involving an adamantyl and a dicarboxy side chain. The 14-3-3 proteins are a family of conserved regulatory molecules found in all eukaryotic cells. They play a crucial role in various cellular processes, including signal transduction, cell cycle regulation, apoptosis, and metabolism. Among the seven known isoforms in mammals, the 14-3-3 ζ/δ isoform stands out due to its unique functions and distribution across different tissues.

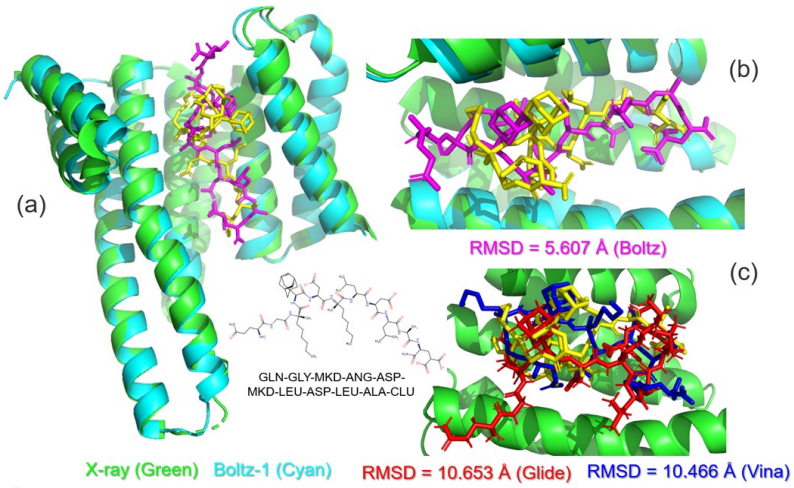

Figure 11. (a) Boltz-1`s prediction of the 3D-structure of the ligand-protein complex between protein 14-3-3ξ and a oligopeptide involving an adamantyl and a dicarboxy side chain. The X-ray structures of 14-3-3ξ, measured at a resolution of 2.34 Å, was obtained from PDB ID: 5JM4 [56]. (b) The overlap of the X-ray and Boltz-1 estimated binding modes of the oligopeptide within the 14-3-3ξ pocket. (c) Comparison of the X-ray binding mode of the peptide (*yellow*) with molecular docking calculations by Glide (*red*) and AutoDock Vina (*blue*).

Macrocyclic scaffolds are commonly found in natural products and are considered promising candidates for developing bioactive macrocyclic peptides aimed at inhibiting protein-protein interactions [57-58]. Recently, novel peptides have been designed that exhibit high affinity for the protein 14-3-3ζ. These peptides incorporate a hydrophobic and a hydrophilic non-natural amino acid into sequences consisting of 11 to 12 residues [56]. Figure 11a shows the X-ray structure of the protein 14-3-3ζ co-crystallized with the oligopeptide with sequence GLN-GLY-MKD-ANG-ASP-MKD-LEU-ASP-LEU-ALA-CLU.

Figure 11 summarizes the benchmarking results for the biomolecular complex between 14-3-3ξ and the adamantane-containing oligopeptide. The Boltz-1 algorithm successfully reproduced protein folding, achieving a RMSD of 0.901 Å (see Table 1). As expected, all three algorithms studied faced challenges in accurately predicting the binding mode (Figures 11b-c). However, while the overall RMSD values were above 5 Å for the three docking tools, Boltz-1 outperformed both Glide and AutoDock Vina in capturing the pharmacophore features of the peptide, positioning the adamantane moiety closer to the X-ray data (Figure 11c).

Conclusions and Future Perspectives

Understanding ligand-protein interactions is essential for advancing drug discovery, protein design, and structural biology. Therefore, modeling ligand-protein interactions is a cornerstone of modern drug discovery and molecular biology, enabling the rational design of therapeutics and a deeper understanding of biological processes [59]. Current commercial tools, such as AlphaFold3, have established a high standard for predicting the 3D structures of biomolecular complexes [6, 60]. However, their accessibility and high costs limit broader adoption. The recently introduced fully open-source model, such as Boltz-1, addresses this issue and competes with these state-of-the-art tools in both accuracy and usability.

We found that Boltz-1 demonstrated strong performance in reproducing protein folding, deriving its capabilities from the parent source code of AlphaFold 3. Boltz-1 effectively reproduces the 3D structures of biomolecular complexes, demonstrating excellent performance, particularly in docking ligands with flexible macrocycles. It successfully re-docked a diverse set of ligands with varying complexities, achieving binding scores comparable to commercial tools such as Glide by Schrodinger. In terms of RMSD ligand-binding ranking, Botlz-1 outperformed the popular docking tool AutoDock Vina for all ligands studied. Finally, while capturing the binding modes of low-molecular-weight organics, predicting complex peptidomimetics remains beyond the current capabilities of Boltz-1. To summarize, our benchmarking indicates that Botlz-1 presents opportunities to improve computational

screening of small molecular libraries and may play a significant role in the future of AI-driven predicting of ligand-protein interactions.

Finally, when our manuscript was ready for submission, Boltz's developing team announced the revolutionizing update for Boltz-2 (https://github.com/jwohlwend/boltz), introducing controllability features including experimental method conditioning, distance constraints, and multi-chain template integration for structure prediction, and the AI model to approach the performance of free-energy perturbation (FEP) methods in estimating small molecule–protein binding affinity.

Acknowledgements

A.V.K. acknowledges the grant № 87/0062 (2021.01/0062) "Molecular design, synthesis and screening of new potential antiviral pharmaceutical ingredients for the treatment of infectious diseases COVID-19" from the National Research Foundation of Ukraine.

References

1. McDonnell R. T., Henderson A. N., Elcock A. H. Structure prediction of large RNAs with AlphaFold3 highlights its capabilities and limitations. *J. Mol. Biol.* **2024**, *436* (22), 168816. https://doi.org/10.1016/j.jmb.2024.168816
2. Kondo H. X., Takano Y. Structure comparison of heme-binding sites in heme protein predicted by alphafold3 and AlphaFold2. *Chem. Lett.* **2024**, *53* (8), upae148. https://doi.org/10.1093/chemle/upae148
3. He X.-h., Li J.-r., Shen S.-y., Xu H. E. AlphaFold3 versus experimental structures: Assessment of the accuracy in ligand-bound G protein-coupled receptors. *Acta Pharm. Sinica* **2025**, 46, 1111–1122 https://doi.org/10.1038/s41401-024-01429-y.
4. Binder J. L., Berendzen J., Stevens A. O., He Y., Wang J., Dokholyan N. V., Oprea T. I. AlphaFold illuminates half of the dark human proteins. *Curr. Opin. Struct. Biol.* **2022**, *74* 102372. https://doi.org/10.1016/j.sbi.2022.102372
5. Zhai S., Liu T., Lin S., Li D., Liu H., Yao X., Hou T. Artificial intelligence in peptide-based drug design. *Drug Discov. Today* **2025**, *30* (2), 104300. https://doi.org/10.1016/j.drudis.2025.104300
6. Duma Y., Kyrychenko A. Benchmarking Google DeepMind's AlphaFold 3 performance for protein 3D-structure prediction. *Kharkiv University Bulletin. Chemical Series* **2024**, *43* (66), 6-25. https://doi.org/10.26565/2220-637X-2024-43-01
7. Wohlwend J., Corso G., Passaro S., Reveiz M., Leidal K., Swiderski W., Portnoi T., Chinn I., Silterra J., Jaakkola T., Barzilay R. Boltz-1 democratizing biomolecular interaction modeling. *bioRxiv* **2024**, 2024.11.19.624167. https://doi.org/10.1101/2024.11.19.624167
8. Goodsell D. S., Morris G. M., Olson A. J. Automated docking of flexible ligands: Applications of AutoDock. *J. Mol. Recognit.* **1996**, *9* (1), 1-5. https://doi.org/10.1002/(SICI)1099-1352(199601)9:1<1::AID-JMR241>3.0.CO;2-6
9. Trott O., Olson A. J. AutoDock vina: Improving the speed and accuracy of docking with a new scoring function, efficient optimization, and multithreading. *J. Comput. Chem.* **2010**, *31* (2), 455-461. https://doi.org/10.1002/jcc.21334
10. Madhavi Sastry G., Adzhigirey M., Day T., Annabhimoju R., Sherman W. Protein and ligand preparation: Parameters, protocols, and influence on virtual screening enrichments. *J. Comput. Aided. Mol. Des.* **2013**, *27* (3), 221-234. https://doi.org/10.1007/s10822-013-9644-8
11. Lu C., Wu C., Ghoreishi D., Chen W., Wang L., Damm W., Ross G. A., Dahlgren M. K., Russell E., Von Bargen C. D., Abel R., Friesner R. A., Harder E. D. OPLS4: Improving force field accuracy on challenging regimes of chemical space. *J. Chem. Theory Comput.* **2021**, *17* (7), 4291-4300. https://doi.org/10.1021/acs.jctc.1c00302
12. Friesner R. A., Banks J. L., Murphy R. B., Halgren T. A., Klicic J. J., Mainz D. T., Repasky M. P., Knoll E. H., Shelley M., Perry J. K., Shaw D. E., Francis P., Shenkin P. S. Glide: A new approach for rapid, accurate docking and scoring. 1. Method and assessment of docking accuracy. *J. Med. Chem.* **2004**, *47* (7), 1739-1749. https://doi.org/10.1021/jm0306430
13. Halgren T. A., Murphy R. B., Friesner R. A., Beard H. S., Frye L. L., Pollard W. T., Banks J. L. Glide: A new approach for rapid, accurate docking and scoring. 2. Enrichment factors in database screening. *J. Med. Chem.* **2004**, *47* (7), 1750-1759. https://doi.org/10.1021/jm030644s

14. Friesner R. A., Murphy R. B., Repasky M. P., Frye L. L., Greenwood J. R., Halgren T. A., Sanschagrin P. C., Mainz D. T. Extra precision Glide: Docking and scoring incorporating a model of hydrophobic enclosure for protein−ligand complexes. *J. Med. Chem.* **2006**, *49* (21), 6177-6196. https://doi.org/10.1021/jm051256o
15. Yang Y., Yao K., Repasky M. P., Leswing K., Abel R., Shoichet B. K., Jerome S. V. Efficient exploration of chemical space with docking and deep learning. *J. Chem. Theory Comput.* **2021**, *17* (11), 7106-7119. https://doi.org/10.1021/acs.jctc.1c00810
16. Tan B., Joyce R., Tan H., Hu Y., Wang J. SARS-CoV-2 main protease drug design, assay development, and drug resistance studies. *Acc. Chem. Res.* **2023**, *56* (2), 157-168. https://doi.org/10.1021/acs.accounts.2c00735
17. Yevsieieva L. V., Lohachova K. O., Kyrychenko A., Kovalenko S. M., Ivanov V. V., Kalugin O. N. Main and papain-like proteases as prospective targets for pharmacological treatment of coronavirus SARS-CoV-2. *RSC Adv.* **2023**, *13* (50), 35500–35524. https://doi.org/10.1039/d3ra06479d
18. Hu Q., Xiong Y., Zhu G.-H., Zhang Y.-N., Zhang Y.-W., Huang P., Ge G.-B. The SARS-CoV-2 main protease (M^{pro}): Structure, function, and emerging therapies for COVID-19. *MedComm* **2022**, *3* (3), e151. https://doi.org/10.1002/mco2.151
19. Lohachova K. O., Sviatenko A. S., Kyrychenko A., Ivanov V. V., Langer T., Kovalenko S. M., Kalugin O. N. Computer-aided drug design of novel nirmatrelvir analogs inhibiting main protease of coronavirus SARS-CoV-2. *J. Appl. Pharm. Sci.* **2024**, *14* (5), 232-239. https://doi.org/10.7324/JAPS.2024.158114
20. Zagórska A., Czopek A., Fryc M., Jończyk J. Inhibitors of sars-cov-2 main protease (M^{pro}) as anti-coronavirus agents. *Biomolecules.* **2024**, *14* (7), 797. https://doi.org/10.3390/biom14070797
21. Yang Y., Luo Y.-D., Zhang C.-B., Xiang Y., Bai X.-Y., Zhang D., Fu Z.-Y., Hao R.-B., Liu X.-L. Progress in research on inhibitors targeting SARS-CoV-2 main protease (M^{pro}). *ACS Omega* **2024**, *9* (32), 34196-34219. https://doi.org/10.1021/acsomega.4c03023
22. Xiao Y.-Q., Long J., Zhang S.-S., Zhu Y.-Y., Gu S.-X. Non-peptidic inhibitors targeting SARS-CoV-2 main protease: A review. *Bioorg. Chem.* **2024**, *147* 107380. https://doi.org/10.1016/j.bioorg.2024.107380
23. Yevsieieva L., Trostianko P., Kyrychenko A., Ivanov V., Kovalenko S., Kalugin O. Design of non-covalent dual-acting inhibitors for proteases M^{pro} and PL^{pro} of coronavirus SARS-CoV-2 through evolutionary library generation, pharmacophore profile matching, and molecular docking calculations. *Sci. Rise. Pharm. Sci.* **2024**, (6(52)), 15-26. https://doi.org/10.15587/2519-4852.2024.313808
24. Yang Y., Cao L., Yan M., Zhou J., Yang S., Xu T., Huang S., Li K., Zhou Q., Li G., Zhu Y., Cong F., Zhang H., Guo D., Li Y., Zhang X. Synthesis of deuterated s-217622 (ensitrelvir) with antiviral activity against coronaviruses including sars-cov-2. *Antivir. Res.* **2023**, *213* 105586. https://doi.org/10.1016/j.antiviral.2023.105586
25. Lohachova K., Sviatenko A., Kyrychenko A., Kalugin O. Evolutionary structure optimization of ensitrelvir as non-covalent inhibitor of SARS-CoV-2 main protease M^{pro}. *Kharkiv University Bulletin. Chemical Series* **2024**, *43* (66), 26-37. https://doi.org/10.26565/2220-637X-2024-43-02
26. Tyagi S., Gupta P., Saini A. S., Kaushal C., Sharma S. The peroxisome proliferator-activated receptor: A family of nuclear receptors role in various diseases. *J. Adv. Pharm. Technol. Res.* **2011**, *2* (4). https://doi.org/10.4103/2231-4040.90879
27. Keil S., Matter H., Schönafinger K., Glien M., Mathieu M., Marquette J.-P., Michot N., Haag-Diergarten S., Urmann M., Wendler W. Sulfonylthiadiazoles with an unusual binding mode as partial dual peroxisome proliferator-activated receptor (PPAR) γ/δ agonists with high potency and in vivo efficacy. *ChemMedChem* **2011**, *6* (4), 633-653. https://doi.org/10.1002/cmdc.201100047
28. Vasquez-Montes V., Rodnin M. V., Kyrychenko A., Ladokhin A. S. Lipids modulate the BH3-independent membrane targeting and activation of Bax and Bcl-xL. *Proc. Natl. Acad. Sci. USA* **2021**, *118* (37), e2025834118. https://doi.org/10.1073/pnas.2025834118
29. Tyagi V., Vasquez-Montes V., Freites J. A., Kyrychenko A., Tobias D. J., Ladokhin A. S. Effects of cardiolipin on the conformational dynamics of membrane-anchored Bcl-xL. *Int. J. Mol. Sci.* **2021**, *22* (17), 9388. https://doi.org/10.3390/ijms22179388

30. Vasquez-Montes V., Kyrychenko A., Vargas-Uribe M., Rodnin M. V., Ladokhin A. S. Conformational switching in Bcl-xL: Enabling non-canonic inhibition of apoptosis involves multiple intermediates and lipid interactions. *Cells* **2020**, *9* (3), 539. https://doi.org/10.3390/cells9030539
31. Rodnin M. V., Kyrychenko A., Vasques-Montes V., Ladokhin A. S. Redesigning apoptotic regulator bid for thrombin activation. *Biopolymers and Cell* **2023**, *39* (4), 257–264. https://doi.org/10.7124/bc.000AA3
32. Li M., Wang D., He J., Chen L., Li H. Bcl-xL: A multifunctional anti-apoptotic protein. *Pharmacol. Res.* **2020**, *151* 104547. https://doi.org/10.1016/j.phrs.2019.104547
33. Kyrychenko A. V., Ladokhin A. S. Fluorescence tools for studies of membrane protein insertion. *Biopolym. Cell* **2018**, *34* (4), 251-271. https://doi.org/10.7124/bc.00097F
34. Lee E. F., Czabotar P. E., Smith B. J., Deshayes K., Zobel K., Colman P. M., Fairlie W. D. Crystal structure of ABT-737 complexed with Bcl-xL: Implications for selectivity of antagonists of the Bcl-2 family. *Cell Death Differ.* **2007**, *14* (9), 1711-1713. https://doi.org/10.1038/sj.cdd.4402178
35. Kim J. G., Shan L. Beyond inhibition: A novel strategy of targeting HIV-1 protease to eliminate viral reservoirs. *Viruses* **2022**, *14* (6), 1179. https://doi.org/10.3390/v14061179
36. Kim E. E., Baker C. T., Dwyer M. D., Murcko M. A., Rao B. G., Tung R. D., Navia M. A. Crystal structure of HIV-1 protease in complex with VX-478, a potent and orally bioavailable inhibitor of the enzyme. *J. Am. Chem. Soc.* **1995**, *117* (3), 1181-1182. https://doi.org/10.1021/ja00108a056
37. Schmitz M., Kaltheuner I. H., Anand K., Düster R., Moecking J., Monastyrskyi A., Duckett D. R., Roush W. R., Geyer M. The reversible inhibitor SR-4835 binds CDK12/cyclin k in a non-canonical G-loop conformation. *J. Biol. Chem.* **2024**, *300* (1). https://doi.org/10.1016/j.jbc.2023.105501
38. Zhang Z., Li Y., Yang J., Li J., Lin X., Liu T., Yang S., Lin J., Xue S., Yu J., Tang C., Li Z., Liu L., Ye Z., Deng Y., Li Z., Chen K., Ding H., Luo C., Lin H. Dual-site molecular glues for enhancing protein-protein interactions of the cdk12-ddb1 complex. *Nat. Commun.* **2024**, *15* (1), 6477. https://doi.org/10.1038/s41467-024-50642-0
39. Wen T., Wang J., Lu R., Tan S., Li P., Yao X., Liu H., Yi Z., Li L., Liu S., Gao P., Qian H., Xie G., Ma F. Development, validation, and evaluation of a deep learning model to screen cyclin-dependent kinase 12 inhibitors in cancers. *Eur. J. Med. Chem.* **2023**, *250* 115199. https://doi.org/10.1016/j.ejmech.2023.115199
40. Houles T., Boucher J., Lavoie G., MacLeod G., Lin S., Angers S., Roux P. P. The CDK12 inhibitor SR-4835 functions as a molecular glue that promotes cyclin k degradation in melanoma. *Cell Death Discovery* **2023**, *9* (1), 459. https://doi.org/10.1038/s41420-023-01754-x
41. Quereda V., Bayle S., Vena F., Frydman S. M., Monastyrskyi A., Roush W. R., Duckett D. R. Therapeutic targeting of CDK12/CDK13 in triple-negative breast cancer. *Cancer Cell* **2019**, *36* (5), 545-558.e7. https://doi.org/10.1016/j.ccell.2019.09.004
42. Ghosh P., Schmitz M., Pandurangan T., Zeleke S. T., Chan S. C., Mosior J., Sun L., Palve V., Grassie D., Anand K., Frydman S., Roush W. R., Schönbrunn E., Geyer M., Duckett D., Monastyrskyi A. Discovery and design of molecular glue enhancers of CDK12–DDB1 interactions for targeted degradation of cyclin *k*. *RSC Chem. Biol.* **2025**, *6* (1), 36-55. https://doi.org/10.1039/D4CB00190G
43. Paterni I., Granchi C., Katzenellenbogen J. A., Minutolo F. Estrogen receptors alpha (ERα) and beta (ERβ): Subtype-selective ligands and clinical potential. *Steroids* **2014**, *90* 13-29. https://doi.org/10.1016/j.steroids.2014.06.012
44. Delfosse V., Grimaldi M., Pons J.-L., Boulahtouf A., le Maire A., Cavailles V., Labesse G., Bourguet W., Balaguer P. Structural and mechanistic insights into bisphenols action provide guidelines for risk assessment and discovery of bisphenol A substitutes. *Proc Natl Acad Sci USA* **2012**, *109* (37), 14930-14935. https://doi.org/10.1073/pnas.1203574109
45. Caenepeel S., Brown S. P., Belmontes B., Moody G., Keegan K. S., Chui D., Whittington D. A., Huang X., Poppe L., Cheng A. C., Cardozo M., Houze J., Li Y., Lucas B., Paras N. A., Wang X., Taygerly J. P., Vimolratana M., Zancanella M., Zhu L., Cajulis E., Osgood T., Sun J., Damon L., Egan R. K., Greninger P., McClanaghan J. D., Gong J., Moujalled D., Pomilio G., Beltran P., Benes C. H., Roberts A. W., Huang D. C., Wei A., Canon J., Coxon A., Hughes P. E. Amg 176, a

selective mcl1 inhibitor, is effective in hematologic cancer models alone and in combination with established therapies. *Cancer Discov.* **2018**, *8* (12), 1582-1597. https://doi.org/10.1158/2159-8290.CD-18-0387

46. Duncan P. I., Stojdl D. F., Marius R. M., Scheit K. H., Bell J. C. The clk2 and clk3 dual-specificity protein kinases regulate the intranuclear distribution of sr proteins and influence pre-mrna splicing. *Exper. Cell Res.* **1998**, *241* (2), 300-308. https://doi.org/10.1006/excr.1998.4083
47. Zhou Q., Lin M., Feng X., Ma F., Zhu Y., Liu X., Qu C., Sui H., Sun B., Zhu A., Zhang H., Huang H., Gao Z., Zhao Y., Sun J., Bai Y., Jin J., Hong X., Zou C., Zhang Z. Targeting clk3 inhibits the progression of cholangiocarcinoma by reprogramming nucleotide metabolism. *J. Experim. Med.* **2020**, *217* (8), e20191779. https://doi.org/10.1084/jem.20191779
48. Onipko O. V., Stoianova V., Buravov O. V., Chebanov V. A., Kyrychenko A., Gladkov E. S. Synthesis of novel derivatives of 4,6-diarylpyrimidines and dihydro-pyrimidin-4-one and *in silico* screening of their anticancer activity. *Curr. Org. Synthesis* **2025**, *22* (4), 556-567. http://dx.doi.org/10.2174/0115701794356958241024082646
49. Goldfeld D. A., Murphy R., Kim B., Wang L., Beuming T., Abel R., Friesner R. A. Docking and free energy perturbation studies of ligand binding in the kappa opioid receptor. *J. Phys. Chem. B* **2015**, *119* (3), 824-835. https://doi.org/10.1021/jp5053612
50. El Daibani A., Paggi J. M., Kim K., Laloudakis Y. D., Popov P., Bernhard S. M., Krumm B. E., Olsen R. H. J., Diberto J., Carroll F. I., Katritch V., Wünsch B., Dror R. O., Che T. Molecular mechanism of biased signaling at the kappa opioid receptor. *Nat. Commun.* **2023**, *14* (1), 1338. https://doi.org/10.1038/s41467-023-37041-7
51. Zheng Z., Huang X.-P., Mangano T. J., Zou R., Chen X., Zaidi S. A., Roth B. L., Stevens R. C., Katritch V. Structure-based discovery of new antagonist and biased agonist chemotypes for the Kappa opioid receptor. *J. Med. Chem.* **2017**, *60* (7), 3070-3081. https://doi.org/10.1021/acs.jmedchem.7b00109
52. Salas-Estrada L., Provasi D., Qiu X., Kaniskan H. Ü., Huang X.-P., DiBerto J. F., Lamim Ribeiro J. M., Jin J., Roth B. L., Filizola M. De novo design of κ-opioid receptor antagonists using a generative deep-learning framework. *J. Chem. Inf. Model.* **2023**, *63* (16), 5056-5065. https://doi.org/10.1021/acs.jcim.3c00651
53. Jamshidi R. J., Sullivan L. C., Jacobs B. A., Chavera T. A., Berg K. A., Clarke W. P. Long-term reduction of kappa opioid receptor function by the biased ligand, norbinaltorphimine, requires c-jun N-terminal kinase activity and new protein synthesis in peripheral sensory neurons. *J. Pharm. Experim. Therapeutics* **2016**, *359* (2), 319-328. https://doi.org/10.1124/jpet.116.235184
54. Larson D. L., Jones R. M., Hjorth S. A., Schwartz T. W., Portoghese P. S. Binding of norbinaltorphimine (norBNI) congeners to wild-type and mutant Mu and Kappa opioid receptors: Molecular recognition Loci for the pharmacophore and address components of Kappa antagonists. *J. Med. Chem.* **2000**, *43* (8), 1573-1576. https://doi.org/10.1021/jm000059g
55. Tyson A. S., Khan S., Motiwala Z., Han G. W., Zhang Z., Ranjbar M., Styrpejko D., Ramos-Gonzalez N., Woo S., Villers K., Landaker D., Kenakin T., Shenvi R., Majumdar S., Gati C. Molecular mechanisms of inverse agonism via κ-opioid receptor–g protein complexes. *Nat. Chem. Biol.* **2025**, https://doi.org/10.1038/s41589-024-01812-0.
56. Krüger D. M., Glas A., Bier D., Pospiech N., Wallraven K., Dietrich L., Ottmann C., Koch O., Hennig S., Grossmann T. N. Structure-based design of non-natural macrocyclic peptides that inhibit protein–protein interactions. *J. Med. Chem.* **2017**, *60* (21), 8982-8988. https://doi.org/10.1021/acs.jmedchem.7b01221
57. Pelay-Gimeno M., Glas A., Koch O., Grossmann T. N. Structure-based design of inhibitors of protein–protein interactions: Mimicking peptide binding epitopes. *Angew, Chem., Int. Ed.* **2015**, *54* (31), 8896-8927. doi: https://doi.org/10.1002/anie.201412070
58. Corbi-Verge C., Garton M., Nim S., Kim P. M. Strategies to develop inhibitors of motif-mediated protein-protein interactions as drug leads. *Annu. Rev. Pharmacol. Toxicol.* **2017**, *57* (Volume 57, 2017), 39-60. doi: https://doi.org/10.1146/annurev-pharmtox-010716-104805
59. Ivanov V., Lohachova K., Kolesnik Y., Zakharov A., Yevsieieva L., Kyrychenko A., Langer T., Kovalenko S. M., Kalugin O. M. Recent advances in computational drug discovery for therapy against coronavirus SARS-CoV-2. *ScienceRise: Pharm. Sci.* **2023**, (6(46)), 4-24. https://doi.org/10.15587/2519-4852.2023.290318

60. Abramson J., Adler J., Dunger J., Evans R., Green T., Pritzel A., Ronneberger O., Willmore L., Ballard A. J., Bambrick J., Bodenstein S. W., Evans D. A., Hung C.-C., O'Neill M., Reiman D., Tunyasuvunakool K., Wu Z., Žemgulytė A., Arvaniti E., Beattie C., Bertolli O., Bridgland A., Cherepanov A., Congreve M., Cowen-Rivers A. I., Cowie A., Figurnov M., Fuchs F. B., Gladman H., Jain R., Khan Y. A., Low C. M. R., Perlin K., Potapenko A., Savy P., Singh S., Stecula A., Thillaisundaram A., Tong C., Yakneen S., Zhong E. D., Zielinski M., Žídek A., Bapst V., Kohli P., Jaderberg M., Hassabis D., Jumper J. M. Accurate structure prediction of biomolecular interactions with AlphaFold 3. *Nature* **2024**, *630* (8016), 493-500. https://doi.org/10.1038/s41586-024-07487-w

Conflict of interest: The authors declare no conflict of interest.

Received 07.05.2025 *Accepted 25.06.2025*

М. В. Прудь[*†], О. В. Кириченко[*]. Вивчення ліганд-білкових взаємодій в епоху штучного інтелекту: оцінка Boltz-1 для прогнозування 3D-структури біомолекулярних комплексів.

[*]*Харківський національний університет імені В.Н. Каразіна, хімічний факультет, майдан Свободи, 4, Харків, 61022, Україна*

[†]*ТОВ «Єнамін», вул. Вінстона Черчилля, 78, м. Київ, 02094, Україна*

Моделювання взаємодій ліганд-білок є надзвичайно важливим у різних наукових та промислових застосуваннях, особливо у розробці лікарських препаратів та структурній біології. Протягом останніх років кілька обчислювальних інструментів на основі штучного інтелекту, таких як AlphaFold 3 та Chai-1r, революціонізували сферу прогнозування біомолекулярних структур. Нещодавно було також представлено відкриту модель глибокого навчання під назвою Boltz-1, що ознаменувалось значним проривом у моделюванні біомолекулярних взаємодій. Щоб оцінити ефективність Boltz-1 у порівнянні з іншими обчислювальними інструментами, ми провели тестування його здатності точно відтворювати 3D-структури різних біомолекулярних комплексів. Ці комплекси включали ферменти та ліганди різної складності, такі як низькомолекулярні органічні ліганди, стероїди та пептидоміметики. Ми виявили, що Boltz-1 продемонстрував високу ефективність у відтворенні згортання білків, досягнувши середньоквадратичного відхилення (RMSD) менше 1 Å. У порівнянні з іншими обчислювальними інструментами, такими як Glide від Schrödinger та AutoDock Vina, здатність Boltz-1 прогнозувати 3D-структури біомолекулярних комплексів була добре збалансованою. Він успішно повторно задокував різноманітний набір лігандів різної складності, досягнувши точностей, порівнянних з показниками комерційного програмного забезпечення Glide. З точки зору RMSD та поз зв'язування лігандів, Boltz-1 перевершив широко використовуваний інструмент для докінгу - AutoDock Vina для всіх оцінених лігандів, демонструючи можливості для поліпшення комп'ютерного скринінгу взаємодій ліганд-білок.

Ключові слова: *згортання білка, фермент, тривимірна структура, дизайн ліків, штучний інтелект, Boltz-1.*

Конфлікт інтересів: автори повідомляють про відсутність конфлікту інтересів.

Надіслано до редакції 07.05.2025 *Прийнято до друку 25.06.2025*